DOI: 10.1002/anie.201305001

Graphene Functionalization

Nickel Cluster Growth on Defect Sites of Graphene: A Computational Study**

*Wang Gao, Jonathan E. Mueller, Josef Anton, Qing Jiang, and Timo Jacob**

The first extraction of graphene in 2004 led to a wide range of experimental and theoretical studies aimed at better understanding and exploiting the unique properties of this novel two-dimensional material.[1] Among the many potential applications, which have been suggested, are uses of graphene as a substrate in high-performance catalysis and as a component in circuit-board technology.

In particular, graphene's high surface area and conductivity have motivated proposals to use it as a substrate for growing and/or anchoring metal nanoparticles in high-performance catalysts and other electrochemical devices.[2,3] However, the activity of such carbon-supported metal catalysts is strongly dependent on the dispersion and stability of the metal clusters on the support (i.e. the ability of the substrate to stabilize metal clusters of various sizes on its surface).[4] Thus, vacancy defects are expected to play a vital role in making graphene suitable for these applications by supplying highly active binding sites for adsorbing and stabilizing metal clusters.

Indeed, finite populations of single and double vacancy defects are thermodynamically stable in graphene, and have been studied extensively.[5–11] Density functional theory (DFT) calculations revealed that vacancy defects resulting from the removal of up to five C atoms reconstruct to form non-hexagonal rings (models are shown in the Supporting Information: Figures S1.b–f).[12] Even larger holes have been observed in electron microscopy experiments.[13]

Defects may also play a critical role in using graphene components for circuit fabrication. For example, taking advantage of the Dirac fermions in graphene requires opening up its band gap to convert it from a conductor into a semiconductor. This conversion can be achieved by doping graphene with either B or N atoms;[14–17] however, another possibility for accomplishing this could be the adsorption of small metal clusters on the surface. Because the adsorption of such clusters can be used to tune additional magnetic and transport properties of the substrate, it might also provide a technique for controlling an additional set of electromagnetic properties.[18]

The catalytic nature of Ni is well established, and Ni nanoparticles are commonly used to catalyze the synthesis of carbon nanostructures. Owing to the strong affinity between Ni and C, the incorporation of Ni atoms into carbon nanostructures, grown using Ni catalysts, has been observed. Ushiro et al. reported that X-ray adsorption measurements detect Ni impurities in carbon nanostructures following nickel-catalyzed synthesis, which even treatment with acid is not able to remove.[19] Moreover, Banhart et al. identified Ni impurities wrapped in onion-like graphenic particles by using electron microscopy.[20] The work of Rinaldi et al. is even more supportive.[21] Combining results from DFT calculations and high-resolution transmission electron microcopy measurements (HR-TEM) utilizing several in situ characterization techniques, they concluded that Ni atoms form very stable Ni–C compounds during nickel-catalyzed carbon nanotube (CNT) growth, which are incorporated into the final products. They also found unexpectedly strong adsorption of the Ni clusters on the CNT supports. However, despite the potential advantages of using Ni nanoparticles adsorbed on graphene, their catalytic and electromagnetic properties (with the exception of single and two Ni atoms adsorbates[22,23]) remain mostly unexplored.

Based on these findings, it would be expected that just as Ni nanoparticles might be used to tailor critical properties of defective graphene sheets, a graphene substrate might be used to modify the catalytic properties of nickel nanoparticles as well. To elucidate this potential interplay we employ DFT to study the adsorption of Ni_n nanoclusters on defective graphene (details in the Supporting Information). As substrate models we select graphene sheets with vacancy defects, resulting from the removal of x atoms (with $x \leq 5$; see Figure S1 in the Supporting Information). To model the adsorbed Ni nanoparticles, we successively grew Ni_n clusters with $n \leq 10$ and focused on the lowest energy adsorption configuration of each Ni_n cluster on each of these six graphene substrates (with and without vacancy defects). The binding energies (referenced against single Ni atoms and the graphene substrate) for the lowest energy configuration are summarized in Figure 1. The binding energies can be explained by three types of bond contributions.

The first type of binding is between Ni atoms. As the cluster size increases the ratio of bulk to surface atoms increases so that the binding energy will asymptotically

[*] Dr. W. Gao, Dr. J. E. Mueller, Dr. J. Anton, Prof. Dr. T. Jacob
Institut für Elektrochemie, Universität Ulm
89081 Ulm (Germany)
E-mail: timo.jacob@uni-ulm.de
Prof. Dr. T. Jacob
Helmholtz Institute Ulm (HIU) Electrochemical Energy Storage
89081 Ulm (Germany)
Prof. Dr. Q. Jiang
School of Materials Science and Engineering, Jilin University
130022, Changchun (China)

[**] We gratefully acknowledge support by the "Deutsche Forschungsgemeinschaft" (DFG) and the "Bundesministerium für Bildung und Forschung" (BMBF) and by the bw-grid for computing resources. Finally, J.E.M. gratefully acknowledges financial support from the Alexander von Humboldt foundation.

Supporting information for this article is available on the WWW under http://dx.doi.org/10.1002/anie.201305001.

 © 2013 Wiley-VCH Verlag GmbH & Co. KGaA, Weinheim

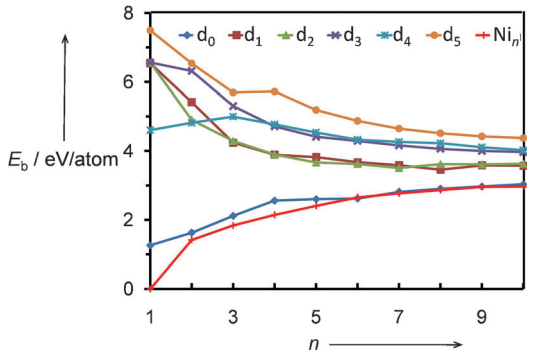

Figure 1. Binding energies (E_b in eV/Ni atom) for the formation of Ni_n clusters in the gas-phase and on graphene substrates with different amounts of vacancy defects (d_0–d_5). The lines guide the eye.

resemble the bulk cohesive energy of Ni (red curve in Figure 1), which we calculated to be 4.61 eV/atom (exp.: 4.44 eV[24]).

The second contribution to the binding comes from attractive interactions between Ni atoms and the conjugated π-system in graphene (Ni–C π-bonds). To separate the contributions of Ni–C and Ni–Ni bonds (which are both included in E_b) it is useful to also define the cluster adsorption energy (E_{ad}), which is referenced to the isolated, fully relaxed Ni cluster and the graphene substrate (details in the Supporting Information). These adsorption energies (Figure S2) suggest that Ni–C π-bonds contribute as much as 1 eV/atom to E_b. The quick increase of the energy gained by forming a Ni–Ni bond (Figure 1, red curve) far outweighs the advantage of having strong Ni–C π-bonds. Thus, the favored location of additional Ni atoms on the d_0 (no defect) substrate is one that enables the formation of strong Ni–Ni bonds on one side of the graphene sheet (Figure 2).

The third contribution to the total binding energy comes from Ni covalently binding to C sp^2 orbitals, which are not involved in the C–C σ-bond network in graphene as a result of a missing C atom at a vacancy defect (e.g. d_1). We refer to these interactions as Ni–C σ-bonds. As can be seen from the large energies (4.5–7.5 eV) associated with the adsorption of a single Ni atom on any of the defective surfaces (d_{1-5}), Ni–C σ-bonds are stronger than either Ni–Ni bonds or Ni–C π-bonds. Thus, their formation is favored, and is the determining factor in cluster growth as long as the C sp^2-orbitals surrounding the defect site are accessible to additional Ni atoms. In maximizing the degree of Ni–C σ-bonding, we find that symmetric clusters, with equal numbers of Ni atoms above and below the defect, are formed. The number of Ni atoms able to participate in Ni–C σ-bonding is naturally related to the size of the defect: 2 Ni atoms for d_1, 4 Ni atoms for d_2 and d_3, 6 Ni atoms for d_4, and 7 Ni atoms for d_5.

In the case of small defects (d_{1-3}) we observe asymmetric cluster growth (beyond the formation of the initial Ni–C σ-bonds). The addition of the first Ni atom that does not participate in Ni–C σ-bonding breaks the symmetry of the cluster, so that there are more atoms on one side of graphene sheet than on the other. The next Ni atom being added can form more Ni–Ni bonds by bonding to this larger cluster.

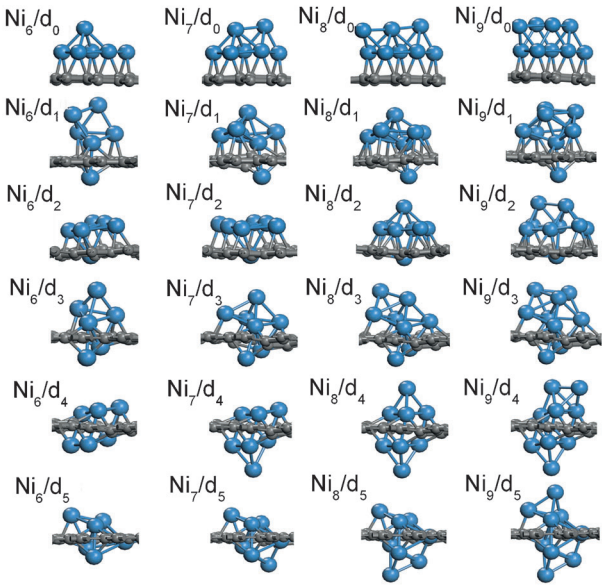

Figure 2. Configurations of Ni clusters on various graphene substrates. d_x denotes the defective graphene with the x atoms removed, which increase from zero in the first row to five in the last row of the figure. Ni_x describes the size of the Ni cluster.

Thus clusters only grow on one side of the sheet where there are small defects.

In the case of larger defects (d_4 and d_5) at least three Ni atoms are able to participate in Ni–C σ-bonding on each side of the surface. Because additional Ni atoms are geometrically hindered from initially coordinating with more than three other Ni atoms, the same number of Ni–Ni bonds will be formed, regardless of which side the Ni atoms are added to. This means that the relative strength of the three new Ni–Ni bonds being formed determines the location at which each new Ni atom is added. This being the case, Ni atoms are preferentially added to the smaller side of the cluster, where the Ni atoms have lower coordination numbers, and as a result are more reactive. Thus, in stark contrast to the growth of asymmetric clusters on only one side of d_1–d_3, we observe the growth of symmetric clusters, with equal numbers of Ni atoms on d_4 and d_5. Because these symmetric clusters grow with one half on either side of the graphene sheet, and thus effectively penetrate the sheet, a stronger binding of both partners is expected. Importantly, the growth of symmetric clusters rationalizes the experimental findings that Ni nanoparticles are very stable on the CNT supports.[21]

The cluster adsorption energies in Figure S2 show that Ni clusters bind relatively weakly to perfect graphene ($E_{ad} \leq 2$ eV) with small variations along the surface plane, indicating that they are likely to diffuse even at room temperature. In contrast, Ni clusters bind strongly to the defective graphene with $E_{ad} \geq 5$ eV, a result of the formation of Ni–C σ-bonds. Moreover, E_{ad} increases as the size of the defect increases.

To better understand the high stability of Ni clusters on defective graphene, we further analyzed the density of states (d-band) of Ni atoms in a bulk Ni_3C (Ni-Ni_3C) solid and in the Ni_9 cluster on the d_5 defect structure (Figure 3). In bulk Ni_3C, every Ni atom binds to two neighboring carbon atoms. In

© 2013 Wiley-VCH Verlag GmbH & Co. KGaA, Weinheim

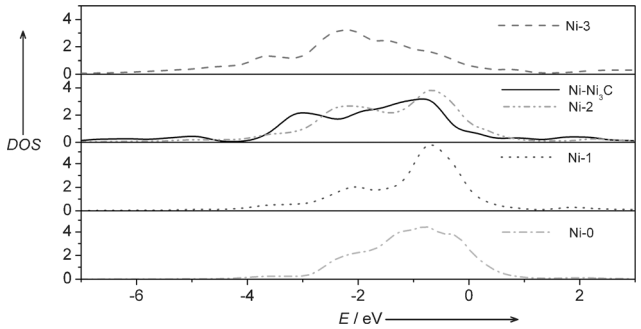

Figure 3. Density of states (d band) for Ni atoms in bulk Ni_3C and Ni_9 cluster on d_5. Ni-3, Ni-2, Ni-1, and Ni-0 denote the Ni atom of Ni_9 cluster involved three, two, one, and zero Ni–C σ-bonds, respectively.

contrast, the Ni atoms in the Ni_9 cluster bind to three, two, one, or even zero carbon atoms (denoted as Ni-3, Ni-2, Ni-1, and Ni-0). As expected, the energies of the d-states associated with each Ni atom reflect the number of Ni–C bonds the Ni atom is directly involved in, with larger numbers of Ni–C bonds corresponding to lower energies (Figure 3). Thus, Ni-3 is more stable than Ni-Ni_3C, forming very stable Ni–C structure on defective graphene and thus supplying a solid foundation for further Ni cluster growth. Indeed, the stable Ni carbide-like compounds have been proposed on Ni surfaces and graphite platelet both experimentally and theoretically.[25,26] Further, stable Ni surface-carbides have been observed during nickel-catalyzed CNT growth by using HR-TEM supported by DFT calculations.[21] Therefore, we expect that, not only graphene but also graphite and CNTs as well as other graphene-like materials (such as graphene oxide and nitrogen-doped graphene), which exhibit interesting catalytic properties,[27–30] should serve as appropriate substrates for Ni cluster growth.

On larger defects (d_{3-5}), E_{ad} increases noticeably with the addition of each Ni atom until the defect's capacity for forming Ni–C σ-bonds is saturated. Thus, these larger defects might be viewed as catalytic sites, which accelerate the nucleation of small clusters. Because E_{ad} is dominated by contributions from Ni–C σ-bonds, it does not change significantly as the size of the Ni cluster increases from Ni_5 up to Ni_{10} (the largest deviation of E_{ad} is 8.47 %). Because the difference in E_{ad} only depends on additional Ni–C π-bonding, the stabilities of Ni_n clusters ($4 \le n \le 10$) on d_3 and d_4 are very similar (the largest deviation in E_{ad} being 12.2 %), and all sizes ranging from Ni_4 to Ni_{10} have similar stabilities on d_3 and d_4 defects. Thus, we expect both the dispersion and stability of Ni clusters on graphene to be substantially enhanced on d_3 and d_4.

To evaluate the stability of the defect-attached nickel clusters, we also calculated the diffusion barriers for Ni_n clusters with $4 < n \le 10$ on d_3 and d_4. Migration of the entire cluster away from the defect requires over 8.5 eV, which indicates a very high stability even at elevated temperatures. As migration of the entire cluster does not seem feasible we also considered step-wise destruction of the attached clusters by removing parts of the cluster only. In this case we still find diffusion barriers above 3.5 eV. The resulting low mobility is in agreement with corresponding experimental observations.[21]

The d-band center (D_c) of the Ni atoms provides a quantitative measure of their catalytic activity.[31,32] Table S1 shows the individual D_c values of the most active Ni atoms in the clusters. The negative shift of the D_c value of the Ni_C atoms (i.e. Ni atoms directly involved in Ni–C σ-bonding), induced by the adsorption on the d_3 and d_4 structures, indicates suppressed reactivity and is most likely due to the formation of Ni–C σ-bonds. In contrast, the D_c values of Ni_{Ni} atoms (i.e. Ni atoms not directly involved in any Ni–C σ-bond) are shifted positively in clusters adsorbed to d_3 and d_4 defects. This enhanced reactivity results from weakened Ni–Ni bonds between Ni_C and Ni_{Ni} atoms as the Ni_C atoms form σ-bonds to C atoms. On d_5, the D_c values of the Ni_C atoms is similar to that of Ni_{Ni} atoms. We explain this similarity by noting that the Ni atom, which replaces the removed C atom, weakens the bond strength between the neighboring C atoms and the surrounding Ni atoms. However, both the Ni_C and Ni_{Ni} atoms in Ni_x/d_5 have a higher reactivity than their counterparts in isolated (i.e. unadsorbed or in gas phase) Ni clusters (as can be seen from the D_c values in Table S1).

For clusters larger than Ni_6, the most reactive atoms are the Ni_{Ni} atoms on d_4. Their D_c values are as much as 0.75 eV higher than in the corresponding isolated Ni clusters ($D_c = -0.85$ eV on Ni_{10}/d_4 and $\rho_{calcd} = -1.60$ eV on Ni_{10}). Therefore, we anticipate that the symmetric structure d_4 would be a good substrate for growing and anchoring Ni catalysts. Given the high reactivity, dispersion, and stability of the Ni clusters on d_3 and d_4, we expect a mixture of d_3 and d_4 defects to be an excellent substrate for improving the catalytic activity of Ni clusters. Interestingly, large holes have indeed been observed by electron microscopy measurements of such substrates.[13] As defects can be generated by irradiation with electrons or ions,[11] modulating the defect size combined with well-selecting particles might indeed be an interesting strategy to tune the catalytic properties.

The band gaps (E_g) associated with various Ni_n/d_x structures for $p(5\times5)$ unit cells are summarized in Table S2. All the graphene sheets except d_2 are metallic, whereas d_2 is a semiconductor with an E_g value of 0.54 eV. To compare our results with other studies, we calculated E_g for the d_2 defect structure in larger unit cells (0.43 eV for $p(8\times8)$ and 0.29 eV for $p(10\times10)$). The latter is close to the value (0.21 eV) calculated for the reconstructed d_2 system in the same unit cell.[33]

As might be anticipated, adsorbed Ni clusters do not strongly influence the band gap of pristine graphene whereas they significantly alter the band gap of defective graphene (except d_2). For example, a single Ni atom on d_3 induces a band gap of 0.49 eV for a $p(5\times5)$ unit cell, changing d_3 from semimetal to semiconductor. It is established that DFT substantially underestimates band gaps. Thus, the E_g value in the actual defective graphene Ni/d_3 is probably much larger than 0.49 eV. The experimentally observed high stability of nickel-atom impurities in carbon species[19–21] suggests that single nickel-atom or nickel-dimer impurities may provide

 © 2013 Wiley-VCH Verlag GmbH & Co. KGaA, Weinheim

a robust means for modulating the band gap of carbon materials.

We attribute this gap modulation to the hybridization states involved in the σ-bonding between the Ni atoms and undercoordinated C atoms. As can be seen in Figure 4a, the

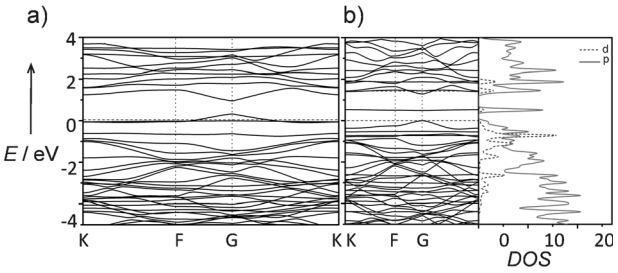

Figure 4. a) Band structure of d_3 and b) band structure and density of states of Ni_1/d_3.

d_3 defect induces the energy band of graphene to shift closer to the Fermi energy. Owing to its asymmetric structure, the energy levels of defective graphene are also less degenerate than those of pristine graphene. Of particular interest is a partially occupied p_z state near the Fermi level, which is split off from the π-band of the carbon ring, and is responsible for the metallic character of d_3. Under the influence of a Ni atom, the graphene p-band states at the bottom of the conduction band mix with Ni d-band states and together split away (from the valence band) to form a separate state directly above the Fermi energy (Figure 4b). As this separated state is now empty and the valence band is fully occupied with the addition of d electrons from the Ni atom, a band gap opens up.

Note that the size of this band gap depends on the concentration of defects, such that the band gap decreases as the concentration of defects decreases on d_0–d_4 (see Table S3). In contrast, E_g values increase on d_5 with decreasing defect concentrations given in monolayers (MLs), defined as the number of defects per unit cell divided by the number of lattice sites per unit cell (e.g. 0.24 eV for Ni_2/d_5 at 1/50 ML in $p(5\times5)$ and 0.37 eV for Ni_2/d_5 at 1/128 ML in $p(8\times8)$). The weak dependence of the size of their band gaps on the defect concentration in the Ni_x/d_5 structures suggests that these structures are promising candidates for applications as graphene-based semiconductors.

In summary, having investigated Ni nanoparticle growth on perfect and defective graphene sheets, we find that Ni clusters grow asymmetrically on only one side of small graphene defects, while they grow symmetrically on larger defects (more than three missing C atoms) forming a nickel carbide layer along the graphene sheet. Increased symmetry of the clusters also corresponds to greater thermodynamic stability, which might improve the catalytic reactivity of the Ni clusters. We anticipate that the Ni_x/d_3 and Ni_x/d_4 structures present optimal catalytic reactivity. Meanwhile, we find that small Ni clusters effectively introduce a band gap into defective graphene, suggesting a possible means of modulating the electronic properties of graphene. In particular, the high thermodynamic stability of Ni_x/d_5 and the weak dependence of the size of its band gap on the defect concentration commend it as a promising candidate for graphene-based semiconductors. Furthermore, our results are helpful for understanding and engineering other carbon-based functionalized materials, such as CNT-based catalysts (e.g. in fuel cells or solar cells) and electronics.[34,35] In particular, it should be possible to use Ni_x/d_n structures to grow graphene–CNT hybrid nanostructures, which have great advantages for practical applications.[36,37]

Received: June 10, 2013
Published online: November 8, 2013

Keywords: carbides · density functional calculations · graphene defects · nanoparticles · semiconductors

[1] K. S. Novoselov, A. K. Geim, S. V. Morozov, D. Jiang, Y. Zhang, S. V. Dubonos, I. V. Grigorieva, A. A. Firsov, *Science* **2004**, *306*, 666–669.
[2] H. L. Wang, J. T. Robinson, G. Diankov, H. J. Dai, *J. Am. Chem. Soc.* **2010**, *132*, 3270–3271.
[3] P. Simon, Y. Gogotsi, *Nat. Mater.* **2008**, *7*, 845–854.
[4] R. Kou, Y. Y. Shao, D. H. Mei, Z. M. Nie, D. H. Wang, C. M. Wang, V. V. Viswanathan, S. Park, I. A. Aksay, Y. H. Lin, Y. Wang, J. Liu, *J. Am. Chem. Soc.* **2011**, *133*, 2541–2547.
[5] J. C. Meyer, C. Kisielowski, R. Erni, M. D. Rossell, M. F. Crommie, A. Zettl, *Nano Lett.* **2008**, *8*, 3582–3586.
[6] J. H. Warner, M. H. Rümmeli, L. Ge, T. Gemming, B. Montanari, N. M. Harrison, B. Büchner, G. A. D. Briggs, *Nat. Nanotechnol.* **2009**, *4*, 500–504.
[7] M. M. Ugeda, I. Brihuega, F. Guinea, J. M. Gómez-Rodríguez, *Phys. Rev. Lett.* **2010**, *104*, 096804.
[8] A. V. Krasheninnikov, P. O. Lehtinen, A. S. Foster, R. M. Nieminen, *Chem. Phys. Lett.* **2006**, *418*, 132–136.
[9] A. A. El-Barbary, R. H. Telling, C. P. Ewels, M. I. Heggie, P. R. Briddon, *Phys. Rev. B* **2003**, *68*, 144107.
[10] G.-D. Lee, C. Z. Wang, E. Yoon, N.-M. Hwang, D.-Y. Kim, K. M. Ho, *Phys. Rev. Lett.* **2005**, *95*, 205501.
[11] F. Banhart, J. Kotakoski, A. V. Krasheninnikov, *ACS Nano* **2011**, *5*, 26–41.
[12] J. M. Carlsson, M. Scheffler, *Phys. Rev. Lett.* **2006**, *96*, 046806.
[13] Ç. Ö. Girit, J. C. Meyer, R. Erni, M. D. Rossell, C. Kisielowski, L. Yang, C.-H. Park, M. F. Crommie, M. L. Cohen, S. G. Louie, A. Zettl, *Science* **2009**, *323*, 1705–1708.
[14] T. B. Martins, R. H. Miwa, A. J. R. da Silva, A. Fazzio, *Phys. Rev. Lett.* **2007**, *98*, 196803.
[15] A. Lherbie, R. X. Blasé, Y. Niquet, F. Triozon, S. Roche, *Phys. Rev. Lett.* **2008**, *101*, 036808.
[16] X. Wang, et al., *Science* **2009**, *324*, 768–771.
[17] L. J. Ci, et al., *Nat. Mater.* **2010**, *9*, 430–435.
[18] J. A. Rodríguez-Manzo, O. Cretu, F. Banhart, *ACS Nano* **2010**, *4*, 3422–3428.
[19] M. Ushiro, K. Uno, T. Fujikawa, Y. Sato, K. Tohji, F. Watari, W. J. Chun, Y. Koike, K. Asakura, *Phys. Rev. B* **2006**, *73*, 144103.
[20] F. Banhart, J. C. Charlier, P. M. Ajayan, *Phys. Rev. Lett.* **2000**, *84*, 686–689.
[21] A. Rinaldi, J.-P. Tessonnier, M. E. Schuster, R. Blume, F. Girgsdies, Q. Zhang, T. Jacob, S. B. A. Hamid, D. S. Su, R. Schlögl, *Angew. Chem.* **2011**, *123*, 3371–3375; *Angew. Chem. Int. Ed.* **2011**, *50*, 3313–3317.
[22] A. V. Krasheninnikov, P. O. Lehtinen, A. S. Foster, P. Pyykkö, R. M. Nieminen, *Phys. Rev. Lett.* **2009**, *102*, 126807.

 © 2013 Wiley-VCH Verlag GmbH & Co. KGaA, Weinheim

[23] E. J. G. Santos, A. Ayuela, D. Sánchez-Portal, *New J. Phys.* **2010**, *13*, 053012.
[24] E. Kaxiras, *Atomic and Electronic Structure of Solids*, Cambridge, Cambridge University Press, **2003**, p. 198.
[25] A. Wiltner, C. Linsmeier, T. Jacob, *J. Chem. Phys.* **2008**, *129*, 084704.
[26] C. F. Sanz-Navarro, P.-O. Åstrand, D. Chen, M. Rønning, A. C. T. van Duin, J. E. Mueller, W. A. Goddard III, *J. Phys. Chem. C* **2008**, *112*, 12663 – 12668.
[27] D. R. Dreyer, R. S. Ruoff, C. W. Bielawski, *Angew. Chem.* **2010**, *122*, 9524 – 9532; *Angew. Chem. Int. Ed.* **2010**, *49*, 9336 – 9344.
[28] D. R. Dreyer, C. W. Bielawski, *Chem. Sci.* **2011**, *2*, 1233 – 1240.
[29] J. R. Potts, D. R. Dreyer, C. W. Bielawski, R. S. Ruoff, *Polymer* **2011**, *52*, 5 – 25.
[30] D. W. Boukhvalov, D. R. Dreyer, C. W. Bielawski, Y.-W. Son, *ChemCatChem* **2012**, *4*, 1844 – 1849.
[31] B. Hammer, J. K. Nørskov, *Surf. Sci.* **1995**, *343*, 211 – 220.
[32] D.-H. Lim, A. S. Negreira, J. Wilcox, *J. Phys. Chem. C* **2011**, *115*, 8961 – 8970.
[33] J. Kotakosiki, A. V. Krasheninnikov, U. Kaiser, J. C. Meyer, *Phys. Rev. Lett.* **2011**, *106*, 105505.
[34] E. Antolini, *Appl. Catal. B* **2009**, *88*, 1 – 24.
[35] M. F. L. De Volder, S. H. Tawfick, R. H. Baughman, A. J. Hart, *Science* **2013**, *339*, 535 – 539.
[36] D. H. Lee, J. E. Kim, T. H. Han, J. W. Hwang, S. Jeon, S.-Y. Choi, S. H. Hong, W. J. Lee, R. S. Ruoff, S. O. Kim, *Adv. Mater.* **2010**, *22*, 1247 – 1252.
[37] V. Sridhar, H.-J. Kim, J.-H. Jung, C. Lee, S. Park, I.-K. Oh, *ACS Nano* **2012**, *6*, 10562 – 10570.

 © 2013 Wiley-VCH Verlag GmbH & Co. KGaA, Weinheim